

Local simulations of common-envelope dynamical inspiral

Impact of rotation, accretion, and stratification (Corrigendum)

Damien Gagnier^{1,2,*}, Giovanni Leidi², Marco Vetter^{1,2}, Robert Andrassy^{1,2}, and Friedrich K. Röpkke^{1,2,3}

¹ Zentrum für Astronomie der Universität Heidelberg, Astronomisches Rechen-Institut, Mönchhofstr. 12-14, D-69120 Heidelberg, Germany
² Heidelberger Institut für Theoretische Studien, Schloss-Wolfsbrunnenweg 35, 69118 Heidelberg, Germany
³ Zentrum für Astronomie der Universität Heidelberg, Institut für Theoretische Astrophysik, Philosophenweg 12, 69120 Heidelberg, Germany

A&A, 707, A1 (2026), <https://doi.org/10.1051/0004-6361/202558057>

1. Corrected force expressions

In Eqs. (22) and (23) of the original paper, the drag and lift forces were computed by projecting the gravitational force density onto directions that varied across the integration volume. The correct expressions project onto fixed unit vectors evaluated at the companion's position, \mathbf{r}_2 . Equations (22) and (23) should respectively read as follows:

$$F_{\text{drag}}(V_i) := - \int_{V_i} \rho \nabla \Phi_2 \cdot \mathbf{e}_\varphi(\mathbf{r}_2) dV$$

$$= \int_{V_i} \frac{\rho G M_2 r \sin \theta \sin \varphi}{h_s^2 v'} \frac{\partial f(v')}{\partial v'} dV \quad (1)$$

and

$$F_{\perp}(V_i) := \int_{V_i} \rho \nabla \Phi_2 \cdot \mathbf{e}_r(\mathbf{r}_2) dV$$

$$= \int_{V_i} \frac{\rho G M_2 (r_2 - r \sin \theta \cos \varphi)}{h_s^2 v'} \frac{\partial f(v')}{\partial v'} dV, \quad (2)$$

where $V_i = \{|\mathbf{r} - \mathbf{r}_2| \leq R_i\}$. Non-rotating simulations were not affected by this error.

2. Updated results

The updated fitting formulas replacing Eq. (36) are the following:

$$\log \frac{F_{\text{drag}}(3\widetilde{R}_a)}{\pi R_a^2 \rho_\infty u_\infty^2} \simeq$$

$$\begin{cases} \sum_{m=0}^2 a_m \mathcal{M}_\infty^{*m} + \frac{a_3}{\sqrt{\mathcal{M}_\infty}} - \frac{a_3}{\sqrt{\mathcal{M}_\infty^*}}, & \mathcal{M}_\infty \leq \mathcal{M}_\infty^*, \\ \sum_{m=0}^2 a_m \mathcal{M}_\infty^m, & \mathcal{M}_\infty > \mathcal{M}_\infty^*, \end{cases} \quad (3a)$$

$$\frac{F_{\perp}(3\widetilde{R}_a)}{\pi R_a^2 \rho_\infty u_\infty^2} \simeq \sum_{m=0}^2 b_m \mathcal{M}_\infty^{m+2}, \quad (3b)$$

Table 1. Updated Table A.1 in Gagnier et al. (2026). Polynomial coefficients a_m and b_m .

Coefficient	Value
a_0	-0.4907848
a_1	0.3147602
a_2	-0.1200657
a_3	-3.817430
b_0	-0.2974315
b_1	-0.04748078
b_2	-0.003452382

where $\mathcal{M}_\infty^* = \mathcal{M}_\infty(\epsilon_\rho = 0.7)$ (see Fig. 4). The updated fitting coefficients are given in Table 1. The lift force prescription now includes three coefficients (b_0 , b_1 , and b_2), replacing the single-coefficient formula of Gagnier et al. (2026).

In the non-stratified regime, the corrected radial force is substantially weaker and reverses sign compared to the values reported in Gagnier et al. (2026) (Fig. 1), while the drag force remains largely unchanged. In the stratified regime, the correction primarily affects the radial force, which is now considerably stronger while still directed inward (Fig. 2), whereas the drag is only mildly affected. The qualitative conclusions of Gagnier et al. (2026) regarding the role of stratification remain unchanged: stratification produces an inward-directed radial force that increases with ϵ_ρ and dominates over the rotation-induced contribution. Since the rotation-induced radial force now also acts inwardly, the two effects reinforce each other, leading to a stronger net inward force than previously reported. As a result, the inspiral trajectories shown in Fig. 3 exhibit a faster orbital decay than in the original paper. Our prescription (Eqs. 3a–3b) still yields a faster inspiral than both the Hoyle–Lyttleton formula and the prescription of De et al. (2020). These corrections further support the conclusion of Gagnier et al. (2026) that the lift force plays a crucial role in the orbital evolution and that it cannot be neglected.

References

De, S., MacLeod, M., Everson, R. W., et al. 2020, *ApJ*, 897, 130
 Gagnier, D., Leidi, G., Vetter, M., Andrassy, R., & Röpkke, F. K. 2026, *A&A*, 707, A1

* Corresponding author: damien.gagnier@uni-heidelberg.de

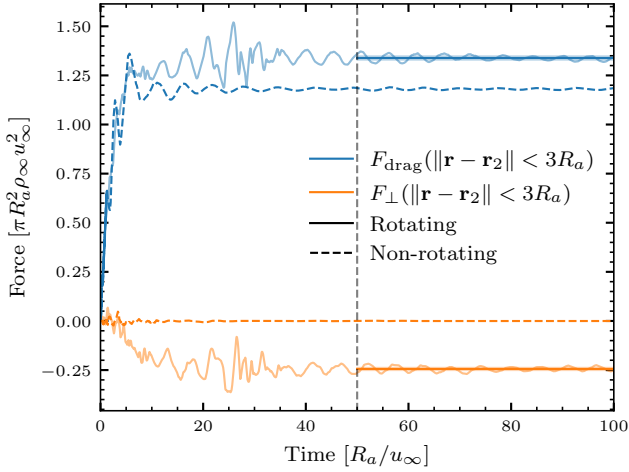


Fig. 1. Updated Figure 6 in Gagnier et al. (2026). Time evolution of the radial and drag forces exerted by the gas on the companion in non-stratified simulations with $Ro = 5.5$ and $\mathcal{M}_\infty = 2$, with and without rotation. Forces were integrated within a sphere of radius $3R_a$. The shaded regions indicate the 3σ range.

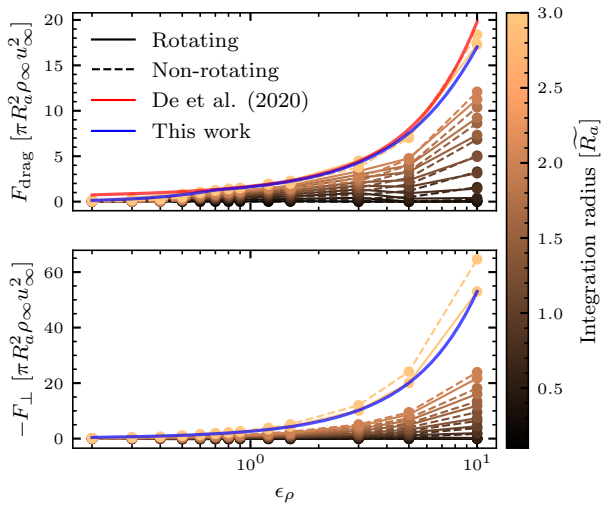


Fig. 2. Updated Figure 8 in Gagnier et al. (2026). Time-averaged drag (top) and lift (bottom) forces on the companion as functions of the stratification parameter ϵ_ρ and integration radius, averaged over $t \in [50, 100] \tilde{R}_a / u_\infty$. The red curve shows the prescription from De et al. (2020, Eq. A4). The blue curve shows our fitting formulae (Eq. 3a).

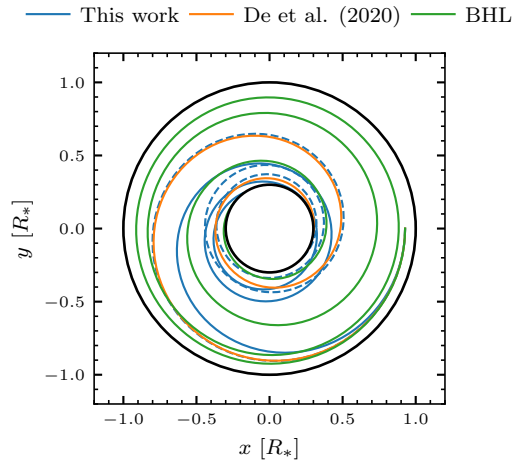


Fig. 3. Updated Figure A.5 in Gagnier et al. (2026). Inspiral of a $0.2 M_\odot$ companion through the envelope of a $2 M_\odot$ red giant, using three drag force prescriptions. The blue curve uses our fitted drag and lift prescriptions (Eqs. 3a–3b); the orange is the prescription from De et al. (2020); the green is the Hoyle–Lyttleton formula, $F_{\text{drag}} = \pi R_a^2 \rho_\infty u_\infty^2$; and the dashed blue curve uses our fitted drag prescription, but F_\perp was set to zero.

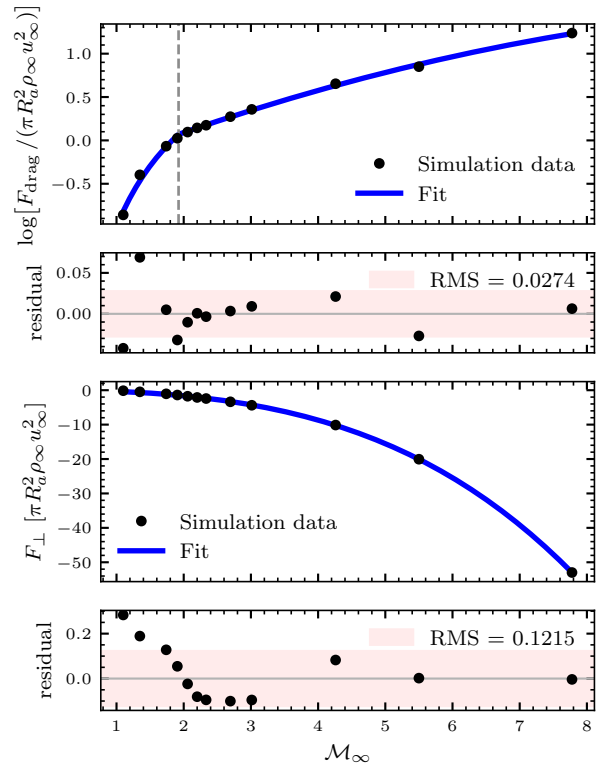


Fig. 4. Fit of the normalized drag and lift forces as a function of \mathcal{M}_∞ using Eq. (3). Black circles denote simulation data and the dashed line marks the critical Mach number \mathcal{M}_∞^* . Lower panels show residuals with a root-mean-square (RMS) error band, defined as $\text{RMS} = \sqrt{\frac{1}{N} \sum_{i=1}^N (y_i - \hat{y}_i)^2}$.